INFLUENCE OF PREPARATION CONDITIONS ON STRUCTURE AND MAGNETIC PROPERTIES OF SOL-GEL DERIVED IRON-DOPED SILOXANE-POLY(ETHYLENEOXIDE) NANOCOMPOSITES

L. A. Chiavacci[1], K. Dahmouche[1], N.J.O. Silva[2], L. D. Carlos[2], V. Amaral[2], V. de Zea Bermudez[3], S.H. Pulcinelli[1], C.V. Santilli[1], V. Briois[4] and A.F. Craievich[5]

[1]Instituto de Química, UNESP, Araraquara-SP, Brazil

[2]Departamento de Física, Universidade de Aveiro, Aveiro, Portugal

[3] Departamento de Química, Universidade de Trás-os-Montes e Alto Douro*, Portugal*

[4]LURE, Université Paris-Sud, Orsay, France

[5] Instituto de Física, USP, São Paulo-SP, Brazil

ABSTRACT

In this work we investigate the effect of hydrochloric acid (HCl) addition on the structure, and thermal and magnetic properties of iron-doped siloxane-polyoxyethylene (POE) hybrids prepared by sol-gel route. X-ray powder diffraction (XRD) and X-ray absorption near edge structure (XANES) results reveal the predominance of ferrihydrite nanoparticles and a mixture of this phase with $FeCl_4^-$ species in the hybrid prepared without and with HCl, respectively. Thermal analysis reveals the existence of two polymeric crystalline phases in the hybrid prepared with HCl, whereas hybrids prepared without HCl are amorphous. The 105 and 60 Å sized ferrihydrite nanoparticles were detected by small-angle X-ray scattering (SAXS) analysis of the composite prepared without and with HCl, respectively. The magnetic results suggest that in both samples antiferromagnetic nanoparticles coexist with small clusters/isolated ions. In the sample without HCl addition, larger particles dominate the magnetic behaviour, while the opposite occurs for the sample prepared using HCl catalyst.

1. Introduction

Extremely versatile siloxane-polyoxyethylene or siloxane-polyoxypropylene hybrids, classed as di-ureasils, have been developed and used as hosts to different doping atoms like Li^+, Na^+, Eu^{3+} to obtain ion-conducting or luminescent materials [1, 2]. In these composites, polyether-based chains of variable lengths are grafted on both ends to a siliceous backbone through urea functionalities. The doping with Fe atom led to hybrid materials where Fe is coordinated to the polymer chains or aggregates into nonoparticles, depending on the iron valence [3-6]. In the case of iron doping hybrid materials the synthesis conditions should be extremely important in the control of size, structure and magnetic properties of iron based nanoparticles. In a recent investigation [6] we have studied the local and nanoscopic structure of iron-doped siloxane-polyoxyethylene nanocomposites prepared by the sol-gel process. This study has revealed the existence of $FeCl_4^-$ species dispersed in the hybrid matrix, resulting from the use of hydrochloric acid (HCl) as a catalyst of the hydrolysis and polycondensation reactions of hybrid precursor molecules. We have established that the proportion of iron-oxy based nanoparticles dispersed in the hybrid matrix increases with doping level. However, the nature of the phase constituting these iron-oxy based nanoparticles and their magnetic properties have not been determined. Furthermore, it seems to be interesting to compare the structure and magnetic behaviour of both sol-gel derived iron-doped nanohybrids prepared with and without HCl catalyst, in order to understand their role on the formation of iron-based phases and to optimise the magnetic properties of these nanocomposites.

The aim of this work is to investigate how the presence of acid catalyst (HCl) affects the structure, the magnetic and the thermal properties of iron(III)-doped siloxane-polyoxyethylene nanocomposites. The study was performed on iron-doped hybrids prepared with and without HCl.

2. Experimental

Iron-doped siloxane-POE hybrid materials were prepared by the sol-gel method, using the procedure described in detail elsewhere [4-6]. In a first step, equimolar amounts of 3-isocyanatopropyltriethoxysilane (Fluka) and a doubly functional amine (Jeffamine-ED®, FLUKA) were stirred together in tetrahydrofuran under reflux for 15 h. This process leads to the hybrid precursor $_3$(OEt)Si-(POE)-Si(OEt)$_3$ with POE molecular weight of 2000g/mol. In a second step, two different samples were prepared by addition of an acid solution of iron(III) nitrate in ethanol/water [H_2O]/[Si] = 2 at molar ratio [O]/[Fe] = 10, ([O] being the ether-type oxygen of POE chains). The first one was obtained by addition of HCl to the iron solution and the second one was prepared without HCl addition. After the addition of iron solution to the hybrid precursor, a transparent sol was obtained. Gelation occurred within 25 min at room temperature. Finally, 0.5 mm thickened monolithic xerogels were obtained after drying the wet gel under vacuum at 80^{o}C for 24 h.

Powder X-ray diffraction (XRD) data were collected on a X'Pert MPD Philips diffractometer with a curved graphite monochromator (CuKα radiation, λ = 1.541 Å). Intensity data were collected by the step counting method (step 0.05º and time 35 s) in a 2θ range between 5 and 70°. The thermal behaviour of hybrids was investigated by Differential Scanning Calorimetry (DSC) measurements carried out on 10 mg samples with scan rate of 10°C/min from –120 to 50°C, using DSC TA Instruments, model 2910.

The nanoscopic structure of the composites was studied by small-angle X-ray scattering (SAXS) measurements. Data collection was done at the synchrotron SAXS beamline of LNLS (Campinas, Brazil), which is equipped with an asymmetrically cut and bent Si(111) monochromator (λ = 1.608 Å) that yields an horizontally focused

beam. A vertical position-sensitive X-ray detector and a multichannel analyzer were used to record the SAXS intensity, I(q), as a function of the modulus of the scattering vector q, $q = (4\pi/\lambda)\sin(\varepsilon/2)$, ε being the scattering angle. The parasitic scattering produced by slits was subtracted from the total scattering intensity. Both scattering intensity were recorded in relative units but, for a quantitative comparison, they were normalised to same experimental conditions and equivalent sample thickness. Since the incident X-ray beam has a point-like cross-section at the detection plane and the width of resolution detector slit was small, no mathematical desmearing of the scattering curves were done.

The X-ray Absorption near edge structure (XANES) spectra corresponding to xerogels with and without HCl were recorded close to the Fe K-edge (7112 eV), at room temperature, using the EXAFS IV spectrometer at LURE (Orsay, France). The spectra were recorded with a 0.25 eV step from 7090 to 7140 eV and with a 0.40 eV step from 7140 to 7210 eV, with a 2 s accumulation time per step, using a Si(311) double-crystal monochromator. Measurements were carried out in transmission mode using as prepared homogeneous pieces of hybrid with appropriate thickness to obtaining a good signal to noise ratio. Pellets of powdered ferrihydrite and $[N(CH_3)_4][FeCl_4]$ were also characterised as reference compounds. The first derivative of the iron foil K-edge spectrum near 7112 eV was used to define the zero of the energy scale. After the pre-edge background subtraction, the XANES spectra were normalised far from the edge, at ≈ 7171 eV.

Sample magnetization M(T,H) was measured with a Quantum Design SQUID magnetometer. The temperature dependence on heating from -268 up to 47°C in zero-field-cooled (ZFC) and field-cooled (FC) procedures at magnetic field H = 50 Oe was measured for the iron doped samples prepared with and without HCl addition. To

determine the magnetic field dependence, hysteresis cycles were measured in the -50 to +50 kOe range at several temperatures from -268 up to -153ºC.

3. Results

Figure 1 shows the XRD patterns of samples prepared with and without HCl addition and of the non-doped hybrid. The broad band centred at 21.9^{o} in all the patterns is associated to the presence of the amorphous siloxane phase. The series of sharp peaks discerned in the patterns of the doped samples at ca. 19.3, 23.2, 26.3, 39.5, 47.2, 48.6 and 49.8^{o} are unequivocally associated with the diffraction of crystalline POE [7]. The other sharp peaks, marked with an asterisk in Fig. 1, are ascribed to a superposition of crystalline POE and ferrihydrite. Moreover, the band at ca. 61.4^{o} (assigned with an arrow in Fig. 1) is clearly attributed to ferrihydrite [8]. The precise identification of the ferrihydrite peaks is achieved recording XDR patterns (not shown) at 50^{o} C, a temperature in which the POE chains are completely amorphous as evidenced by DSC shown in Figure 2.

The DSC curves (Fig. 2) correspond to the iron-doped hybrids prepared with and without HCl addition compared to that of undoped sample. The glass transition temperature, observed at -103ºC for the undoped sample, shifts to -61 and -53ºC with iron doping, being higher for the hybrids prepared in presence of HCl. The undoped hybrid presents a crystallisation and a melting peak of POE chains centred at -40 and 25ºC, respectively. For the doped hybrid prepared with HCl a broad crystallisation peak at -25ºC and two endothermic peaks centred at 28 and 40ºC are observed. For the sample prepared without HCl no peaks associated to the crystallisation and melting were evidenced in the DSC curve.

The SAXS patterns corresponding to both iron-doped nanocomposites, prepared with and without HCl, are displayed in Figure 3. The low q-range of the experimental results can be well-fitted by the Guinier equation [9], that describes the asymptotic behaviour at small q of the scattering intensity produced by a isotropic and dilute set of isolated colloidal particles embedded in a homogeneous matrix. Guinier equation, for a simple two-electron density model, is given by:

$$I(q) = N(\rho_p - \rho_m)^2 \langle V^2 \rangle . e^{-\frac{1}{3}R_G q^2} \qquad (1)$$

where N is the number of particles in the irradiated sample, ρ_p and ρ_m are the electron densities of the particles and the matrix, respectively, $<V^2>$ is the average of the particle square volume and R_G is named as Guinier average of the radii of gyration, r_g, of the particles. For a set of particles containing a distribution of radii of gyration, R_G is larger than the arithmetic average $<r_g>$, i. e. its value is biased towards the radius of gyration of the largest particles.

The inset in Fig. 3 exhibits log I(q) versus q^2 plots of the scattering intensity of both samples, which displays the linear behaviour expected from Guinier equation. The magnitude of the slope of the straight line and so the R_G corresponding to the doped hybrid prepared with HCl is clearly lower than that from the sample without HCl. The R_G values of the particles dispersed in the hybrid prepared with and without HCl are 60 and 105 Å, respectively.

The SAXS intensity curve corresponding to the doped hybrid without HCl (Fig. 3, top) has a rather strong a q-independent part that is not expected from a two-electron density model. This contribution is generally related to the existence of density fluctuations inside the major phase that yield a nearly constant contribution to

the scattering intensity. This constant intensity is not apparent, or is much weaker, in the scattering intensity produced by the doped hybrid with HCl.

Figure 4 shows the XANES spectra for the iron-doped samples prepared with and without HCl addition compared with the ferrihydrite and $N(CH_3)_4FeCl_4$ reference compounds. For the iron-doped samples the XANES spectra display a small pre-edge structure and an intense broad white line characteristic of a distorted octahedral symmetry around the metal. The XANES spectra of the sample prepared in absence of HCl is similar to the one reported for the ferrihydrite reference. On the other hand, the shape of spectrum of doped sample prepared in presence of HCl seems to be intermediary between that of ferrihydrite and $N(CH_3)_4FeCl_4$, suggesting the presence of a mixture of different iron-based species. We can rebuild the XANES spectrum of the sample prepared with HCl considering a linear combination of the XANES spectrum of the $N(CH_3)_4FeCl_4$ reference and of the XANES spectrum of the hybrid prepared without HCl. An example of fit is illustrated in Fig. 4 and leads to 15% of $FeCl_4^-$.

The temperature dependence of the magnetic susceptibility on heating from -268 up to 47°C in ZFC and FC procedures is shown in Figure 5. For each sample, the upper curve corresponds to the FC procedure. For both samples, thermal irreversibility is observed below about -233°C. The blocking effect associated with the presence of magnetic nanoparticles manifests on the thermal irreversibility, being much stronger on the sample prepared without HCl addition. Moreover, a clear maximum on the ZFC curve is observed at T = -241°C, while on the sample prepared with HCl only a small shoulder is apparent at approximately the same temperature.

4. Discussion

The first result to be noticed is the clear difference between the qualitative features of the SAXS curves corresponding to undoped and iron-doped hybrids. SAXS curves corresponding to undoped hybrids are dominated by the scattering produced by siloxane-based clusters embedded in the polymeric phase [6]. These clusters are relatively small (size of about 10 Å) and spatially correlated so that the scattering curves exhibit a clear and characteristic interference peak. The existence of a maximum intensity at q = 0 and the absence of any correlation peak in the SAXS patterns from both doped samples suggest that colloidal particles other than siloxane-based clusters are formed. Based on the XRD (Fig. 1) and XANES (Fig. 4) results and in the absence of any interference peak in SAXS curves (Fig. 3), we have concluded that a set of spatially uncorrelated ferrihydrite nanoparticles with a size of about 50-100 Å are formed in both doped samples.

The presence of a significant number of iron-based nanoparticles explains the absence of apparent effects of siloxane clusters in the SAXS curves (Fig. 3). As a matter of fact, the electron density contrast factor in Eq. 1, $(\rho_p-\rho_m)^2$, of the iron-based particles and the polymer matrix is expected to be much higher than the contrast factor associated with siloxane clusters. In addition, the volume of the iron-based nanoparticles is much higher than siloxane clusters. Both arguments justify why the relevant features of the scattering intensity from iron-doped hybrids are so different from those produced by undoped samples. Furthermore, the larger radii of gyration of the iron-based nanoparticles in the composite prepared without HCl (R_G = 105Å) compared with the hybrid prepared with HCl (R_G = 60Å) indicates that the increase of the acidity of the medium by adding HCl has an efficient role in the control of the hydrolysis and condensation reaction of the iron precursor. The presence of $FeCl_4^-$

species suggested by XANES (Fig. 4) and confirmed by EXAFS [11], coupled to the acidity of the medium may result in more stable coordination sphere, difficulting the hydrolysis reaction. This feature suggests that the size of ferrihydrite nanoparticles embedded in the hybrid matrix can be changed in a controlled way by adjusting the amount of HCl.

The presence of $FeCl_4^-$ species in the hybrid prepared using HCl has also an influence on the thermal properties of the hybrid materials (Fig. 2). The change of the organic phase crystallisation temperature, which occurs around -40ºC in the undoped composite increases up to -25ºC when doping is done in presence of HCl, revealing that the structure of the crystalline polymer phase is modified in such synthesis conditions. The two endothermic peaks centred at 28 and 40ºC can be attributed to the occurrence of two melting processes associated to the presence of two crystalline polymer phases. One of the melting processes occur at the same temperature (28º C) observed for the undoped hybrid, indicating that this crystalline POE phase has similar structure in both doped or undoped samples. As the melting of the more stable crystalline phase (40ºC) is verified only in the presence of HCl, we suggest that this phase is formed by the reaction between POE chain and $FeCl_4^-$ species. The amorphous character of the hybrid prepared without HCl and the marked thermal stability (up to 40° C) of the crystalline phase of the composite prepared using HCl, leads to an interesting effect on the mechanical properties of the materials: at ambient temperature the sample prepared without HCl present a high flexibility comparable to a rubber, while the hybrid prepared using HCl exhibits a high fragility, like a glass. Furthermore, the increase of the glass transition temperature by doping indicates that the mobility of the POE chains decreases. This effect is more pronounced for the iron-doped-hybrid prepared with HCl.

The above mentioned strong difference in the structure of the polymeric matrix of the hybrids prepared with and without HCl explains one of the relevant features of the SAXS curves plotted in Fig. 3 (above), namely the existence of a strong constant contribution to the intensity from the sample prepared without HCl, while the same contribution is not apparent in the curve from the sample with HCl (Fig. 3, below). Amorphous structures have inherent and rather strong density fluctuations that are not present in crystalline materials. Even though the crystallinity of the matrix in the sample prepared with HCl is not perfect, the density fluctuations in the matrix are significantly weaker and, consequently, their contribution to the constant part of the SAXS intensity is expected to be, as experimentally verified, much lower.

On the ZFC curve (Fig. 5) of the sample with HCl, below -233ºC, the Curie law-type susceptibility (and its temperature dependence) suggests the dominance of a large fraction of Fe ions in very small clusters or nearly isolated, coexisting with some blocked nanoparticles. Such small clusters can also be present in the sample without HCl but only in very small amounts. The magnetic field dependence M(H) (shown in the, for T = -268ºC) clarifies such bimodal interpretation. The magnetic field dependence M(H) (shown in the inset of Fig. 5, for T = -268^{o}C) clarifies such bimodal interpretation. At low temperatures (below -233^{o}C, the blocking temperature of the larger particles) the fit with a Langevin modified function, allowed the determination of the magnetic moment, μ, associated with the small cluster/ nearly isolated Fe ions. In both samples, at -268°C, μ is of the order of 10 μ_B corresponding to clusters with about 3 uncompensated Fe ions. The saturation magnetization, M_s which is also obtained from the fit, is given by the product of the number of small clusters, N_c, by μ. On the sample with HCl, M_s and consequently N_c is more than 10 times greater than in the sample without HCl. At T = -268^{o}C, the sample without HCl displays coercive

and exchange fields of the order of 1000 Oe, rapidly decreasing with temperature, an indication of the existence of nanoparticles with antiferromagnetic interactions. These values and characteristic temperature dependences are similar to the ones found for ferrihydrite nanoparticles in an analogous organic-inorganic matrix [5]. The sample with HCl displays exchange fields of about 100 Oe and negligible coercive fields, consistent with much less developed AF nanoparticles. Above T = -233^{o}C, the M(H) curves are dominated by the larger nanoparticles features. Accordingly, in the sample without HCl one obtains $\mu = 160\ \mu_B$, yielding an estimation of 50 uncompensated Fe^{3+} ions.

5. Conclusion

This study has shown that the presence of HCl during the synthesis of sol-gel derived iron-doped siloxane-polyoxyethylene nanocomposites affects their structure, magnetic and thermomechanic properties. In particular, this study evidences the possibility to control the average size of the ferrihydrite nanoparticles dispersed in the hybrid matrix and consequently their magnetic properties by controlling the amount of HCl used in the synthesis procedure. The magnetic results evidences that in both samples antiferromagnetic nanoparticles coexist with small clusters/isolated ions. In the sample without HCl addition, larger particles dominate the magnetic behaviour while the opposite occurs for the sample prepared using HCl catalyst. Magnetic nanocomposites prepared without HCl are flexible like rubbers, or fragile like glasses when prepared in presence of HCl.

Acknowledgments: Authors acknowledge the Brazilian agencies CAPES, CNPq and FAPESP and the ICCTI (Portugal) for the financial supports.

6. References

[1] J. A. Chaker, K. Dahmouche, C. V. Santilli, V. Briois, A. M. Flank, S. H. Pulcinelli, P. Judeinstein, J. Non-Cryst. Solids **304** (2002) 109.

[2] L. D. Carlos, R. A. Sá Ferreira, V. de Zea Bermudez, C. Molina, L. A. Bueno, S. J. L. Ribeiro, Phys. Rev. B **60** (1999) 10042.

[3] N. J. O. Silva, K. Dahmouche, C. V. Santilli, V. S. Amaral, L. D. Carlos, V. de Zea Bermudez, A. F. Craievich, J. Appl. Cryst. **36** (2003), in press.

[4] N. J. O. Silva, V. S. Amaral, L. D. Carlos, V. de Zea Bermudez, J. Appl. Phys. **93** (2003) 6978.

[5] V. S. Amaral, L. D. Carlos, N. J. O. Silva, V. de Zea Bermudez, K. Dahmouche, C. V. Santilli, A. F. Craievich, F. Palacio, "*Hybrid Organic-Inorganic Materials"*, (Matter. Res. Soc. Proc. Pittsburgh, PA) **726** (2002) 143.

[6] L. A Chiavacci, K. Dahmouche, V. Briois, C. V. Santilli, V. de Zea Bermudez, L. D. Carlos, J. P. Jolivet, S. H. Pulcinelli, A. F. Craievich, J. Appl. Cryst. **36** (2003) 405.

[7] L. D. Carlos, V. De Zea Bermudez, R. A. Sá Ferreira, L. Marques, M. Assunção, Chem. Mater. **11** (1999) 581.

[8] J. L. Jambor, J. E. Dutrizac, Chem. Rev. **98** (1998). 2549.

[9] A. Guinier, *"Théorie et Technique de la Radiocristallographie",* (1964) Eds. Dunod (Paris)

FIGURE CAPTIONS

Figure 1. Room temperature (25ºC) X-ray powder diffraction of iron-doped siloxane-POE hybrid prepared with and without addition of HCl. The pattern of the non-doped di-ureasil sample is also included. The meaning of the asterisk and arrow is discussed in the text.

Figure 2. DSC curves for undoped siloxane-POE hybrid and for iron-doped hybrids prepared with and without HCl.

Figure 3. SAXS curves corresponding to iron-doped hybrids prepared with (down curve) and without (upper curve) HCl. The Guinier plot is shown in the inset for both samples.

Figure 4. XANES spectra of iron-doped hybrids prepared with and without HCl coupled to that of references compounds

Figure 5. Temperature dependence of the magnetic susceptibility of iron-doped hybrids, measured after field cooling (FC) and zero-field cooling (ZFC). The inset shows the field dependence of the magnetization for the two hybrids at T = -268ºC.

Figure 1

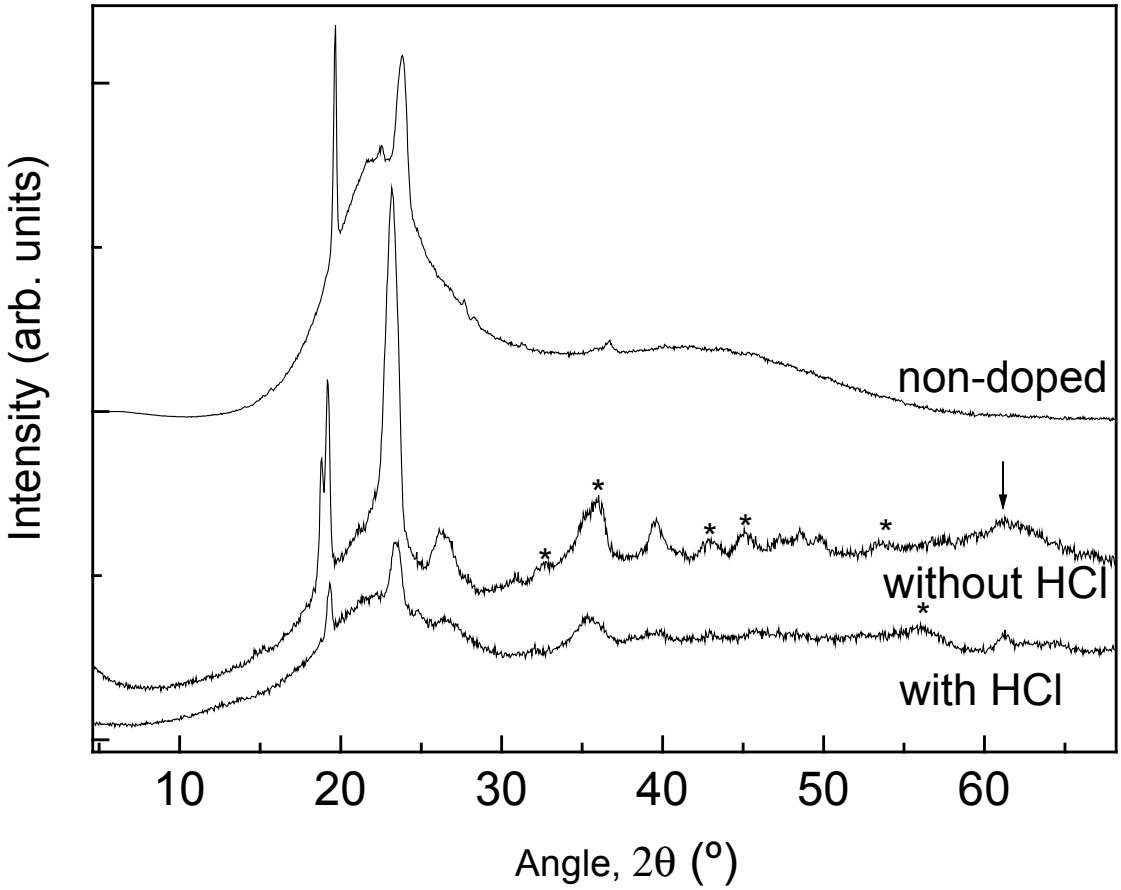
Intensity (arb. units)
non-doped
without HCl
with HCl
10
20
30
40
50
60
Angle, 2θ (º)

Figure 2

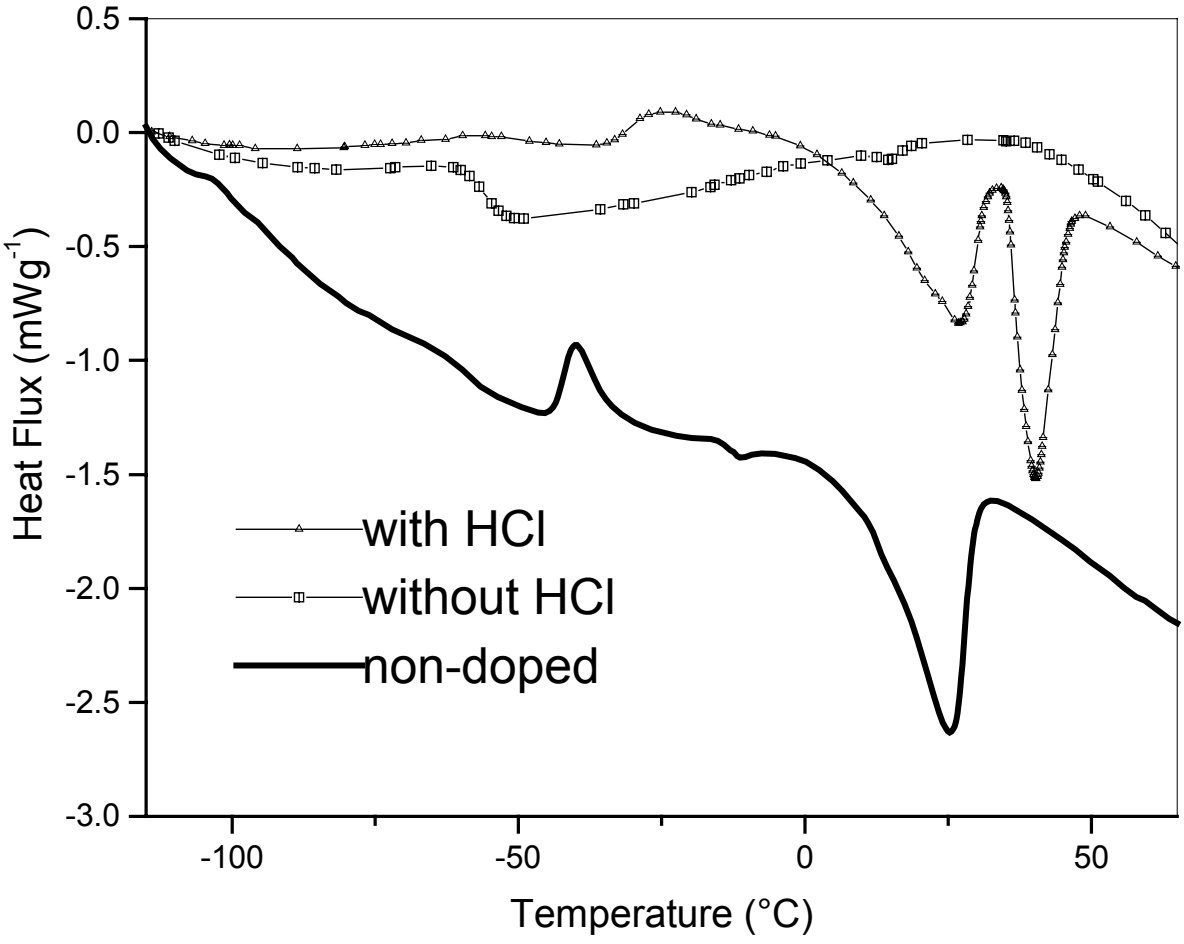
0.5
0.0
-0.5
-1.0
-1.5
-2.0
-2.5
-3.0
Heat Flux (mWg-1)
-100
-50
0
50
Temperature (°C)
with HCl
without HCl
non-doped

Figure 3

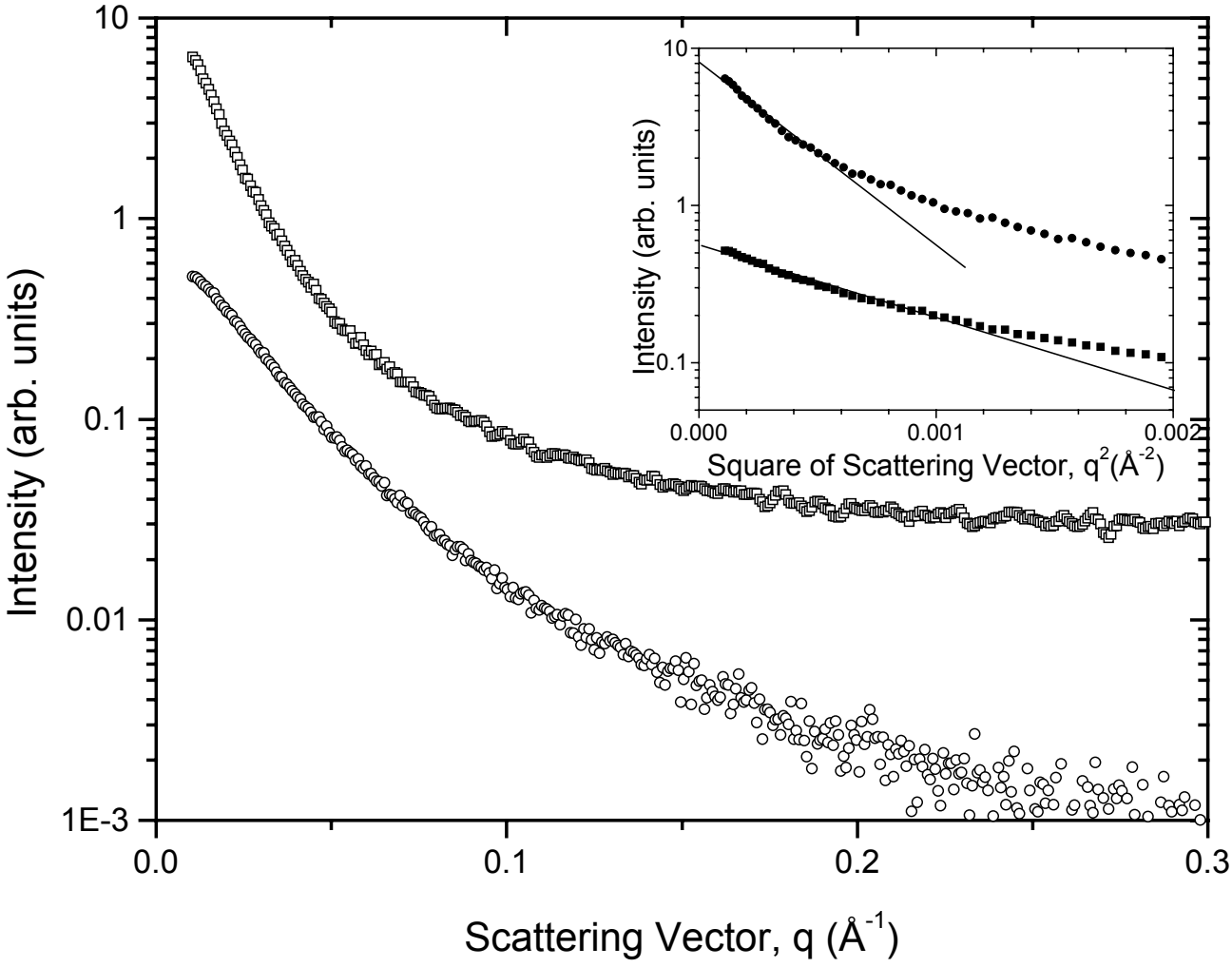
10
1
0.1
0.01
1E-3
0.0
0.1
0.2
0.3
Intensity (arb. units)
Scattering Vector, q (Å^{-1})
10
1
0.1
0.000
0.001
0.002
Intensity (arb. units)
Square of Scattering Vector, q^2(Å^{-2})

Figure 4

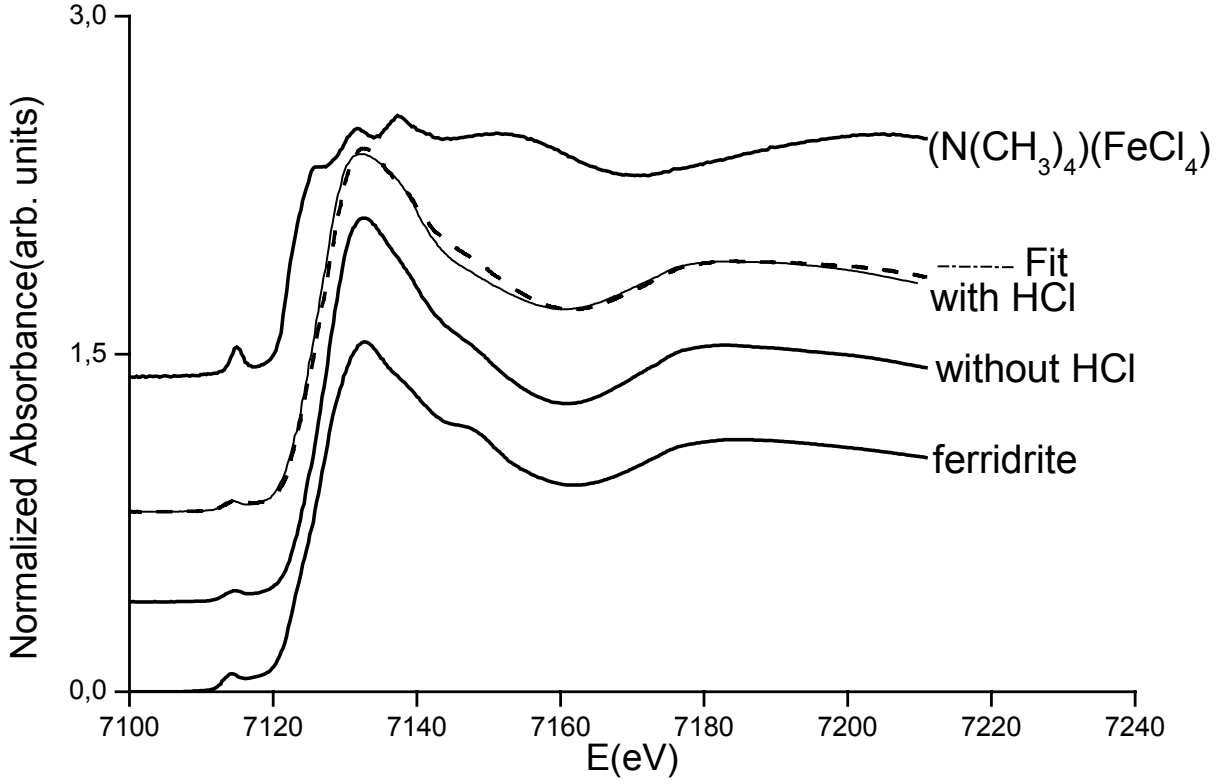
3,0
1,5
0,0
Normalized Absorbance(arb. units)
7100
7120
7140
7160
7180
7200
7220
7240
E(eV)
(N(CH3)4)(FeCl4)
Fit
with HCl
without HCl
ferridrite

Figure 5

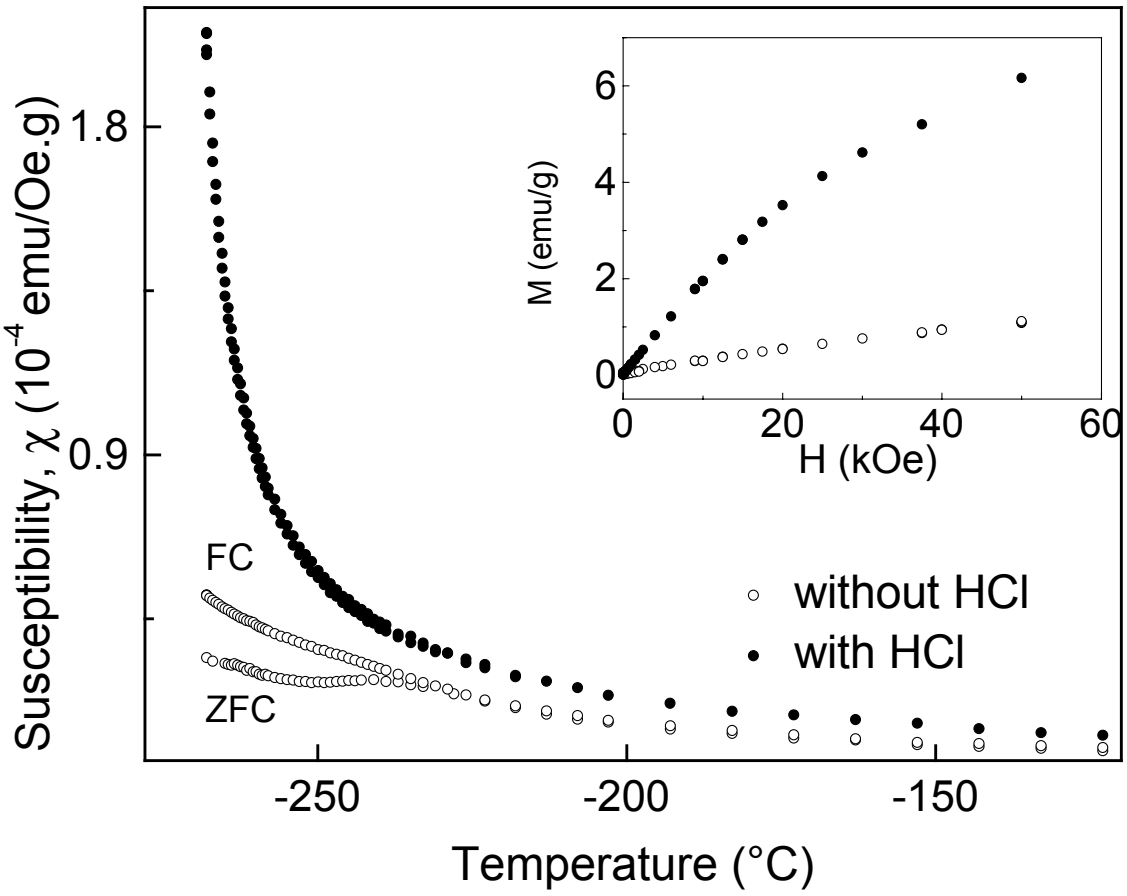
Susceptibility, χ (10^-4 emu/Oe.g)
1.8
0.9
-250
-200
-150
Temperature (°C)
FC
ZFC
without HCl
with HCl
M (emu/g)
6
4
2
0
0
20
40
60
H (kOe)